



*Supplement of*

**Impact of fossil and non-fossil fuel sources on the molecular compositions of water-soluble humic-like substances in PM<sub>2.5</sub> at a suburban site of Yangtze River Delta, China**

Mengying Bao et al.

*Correspondence to:* Yan-Lin Zhang ([dryanlinzhang@outlook.com](mailto:dryanlinzhang@outlook.com))

The copyright of individual parts of the supplement might differ from the article licence.

1    **Sections**

2    **S1.** FT-ICR MS data processing

3

4    **Tables**

5    **Table S1.** Relative intensity weighted average values of number, molecular weight ( $MW_w$ ),  
6    elemental ratios ( $O/C_w$ ,  $H/C_w$ ), double-bond equivalent ( $DBE_w$ ), aromaticity index ( $AI_w$ ), and  
7     $DBE/C_w$  of different elemental category of assigned formulas in summer.

8    **Table S2.** Relative intensity weighted average values of number, molecular weight ( $MW_w$ ),  
9    elemental ratios ( $O/C_w$ ,  $H/C_w$ ), double-bond equivalent ( $DBE_w$ ), aromaticity index ( $AI_w$ ), and  
10    $DBE/C_w$  of different elemental category of assigned formulas in winter.

11   **Table S3.** Classification basis of Van Krevelen diagram.

12   **Table S4.** Statistics on S-containing compounds based on O/S in summer.

13   **Table S5.** Statistics on S-containing compounds based on O/S in winter.

14

15   **Figures**

16   **Figure S1.** 48-h backward trajectories in summer (left) and winter (right).

17   **Figure S2.** FT-ICR mass spectra of 6 samples in summer.

18   **Figure S3.** FT-ICR mass spectra of 6 samples in winter.

19   **Figure S4.** Number percentage of aliphatic ( $AI=0$ ), olefinic ( $0 < AI \leq 0.5$ ) and aromatic ( $AI > 0.5$ )  
20   formulas in CHO, CHON, CHOS and CHONS compounds in summer.

21   **Figure S5.** Number percentage of aliphatic ( $AI = 0$ ), olefinic ( $0 < AI \leq 0.5$ ) and aromatic ( $AI > 0.5$ )  
22   formulas in CHO, CHON, CHOS and CHONS compounds in winter.

23   **Figure S6.** Number percentage of formulas for different carbon atom numbers (a) and total relative  
24   intensity of formulas for different carbon atom numbers (b) in CHO compounds in summer and  
25   winter.

26   **Figure S7.** Time series of the relative intensities of typical CHO compounds in biomass burning  
27   organic aerosols (BBOA) ((a), (b), (c), (d) and (e)) and the mass concentrations of levoglucosan  
28   (f).

29   **Figure S8.** Distribution of the relative intensities of OSs from different precursors.

30

31   **References**

32 S1. FT-ICR MS data processing

33 The molecular formulas assignment was performed using a custom software for the signals  
34 with a signal-to-noise ratio above 10 with a mass tolerance of  $\pm 1$  ppm. Each molecular formula  
35 ( $C_cH_hO_oN_nS_s$ ) contained certain elements where C, H, O, N, and S represented the element carbon,  
36 hydrogen, oxygen, nitrogen, and sulfur and c, h, o, n, and s corresponded to the number of C, H,  
37 O, N, and S atoms, respectively. Both the O/C and H/C ratios were limited to 0-3. The formulas  
38 identified which contained isotopomers (i.e.,  $^{13}C$ ,  $^{18}O$ , or  $^{34}S$ ) were not discussed in this study. The  
39 maximum number of atoms for each formula was set as 60 for  $^{12}C$ , 60 for  $^1H$ , 20 for  $^{16}O$ , 2 for  $^{14}N$ ,  
40 and 2 for  $^{32}S$ , respectively. The double bond equivalents (DBE) were calculated as follows to  
41 estimate the unsaturation degree of each formula:  $DBE = (2c+2-h+n)/2$ . The aromatic index (AI)  
42 which can reflect the degree of aromaticity were calculated following the equation:  $AI = (1+c-0.5o-$   
43  $s-0.5h)/(c-0.5o-s-n)$  (Koch and Dittmar, 2006; Kroll et al., 2011). There may be aromatic ring  
44 structures in the compounds if  $AI > 0.5$  and condensed aromatic structures may exist if  $AI \geq 0.67$ .  
45 The AI values were treated as zero if the calculated AI values were negative.

46 The relative intensity weighted elemental ratios, DBE, AI, and molecular weight were  
47 calculated following the equations (Jiang et al., 2020; Song et al., 2018):

48  $O/C_w = \sum(Ini * O/C_i) / \sum Ini$

49  $H/C_w = \sum(Ini * H/C_i) / \sum Ini$

50  $O/N_w = \sum(Ini * O/N_i) / \sum Ini$

51  $O/S_w = \sum(Ini * O/S_i) / \sum Ini$

52  $DBE_w = \sum(Ini * DBE_i) / \sum Ini$

53  $DBE/C_w = \sum(Ini * DBE/C_i) / \sum Ini$

54  $AI_w = \sum(Ini * AI_i) / \sum Ini$

55  $MW_w = \sum(Ini * MW_i) / \sum Ini$

56 Where  $Ini$  represents the intensity for each individual molecular formula and  $O/C_i$ ,  $H/C_i$ ,  $O/N_i$ ,  
57  $O/S_i$ ,  $DBE_i$ ,  $DBE/C_i$ ,  $AI_i$ , and  $MW_i$  represents the  $O/C$ ,  $H/C$ ,  $O/N$ ,  $O/S$ ,  $DBE$ ,  $DBE/C$ ,  $AI$ , and  $MW$   
58 of the molecular formula i.

59 Table S1. Relative intensity weighted average values of number, molecular weight ( $MW_w$ ),  
 60 elemental ratios ( $O/C_w$ ,  $H/C_w$ ), double-bond equivalent ( $DBE_w$ ), aromaticity index ( $AI_w$ ), and  
 61  $DBE/C_w$  of different elemental category of assigned formulas in summer.

Samples (Sampling time)	Elemental compositions	Number of Formulas	$MW_w$	$O/C_w$	$H/C_w$	$DBE_w$	$AI_w$	$DBE/C_w$
S1 (2017/8/20)	Total	2369	354.83	0.72	1.39	6.01	0.28	0.41
	CHO	537	376.37	0.47	1.20	8.52	0.28	0.46
	CHON	958	382.72	0.64	1.28	7.86	0.26	0.48
	CHOS	454	314.61	0.78	1.52	3.77	0.12	0.34
	CHONS	420	344.90	0.99	1.59	3.81	0.49	0.37
	Total	2151	336.51	0.80	1.46	4.92	0.28	0.39
S2 (2017/8/21)	CHO	427	362.98	0.56	1.15	7.95	0.29	0.49
	CHON	598	353.76	0.71	1.23	7.38	0.33	0.52
	CHOS	566	314.26	0.76	1.53	3.73	0.13	0.34
	CHONS	560	337.01	0.98	1.65	3.49	0.39	0.35
	Total	3781	365.72	0.63	1.43	5.65	0.20	0.38
S3 (2017/8/22)	CHO	750	384.47	0.48	1.24	7.86	0.26	0.44
	CHON	1308	397.69	0.59	1.26	7.85	0.28	0.48
	CHOS	919	335.46	0.60	1.54	4.13	0.09	0.32
	CHONS	804	362.69	0.82	1.60	4.01	0.22	0.34
	Total	4046	387.91	0.61	1.42	6.21	0.22	0.38
S4 (2017/8/23)	CHO	889	396.83	0.45	1.30	7.72	0.23	0.40
	CHON	1722	424.46	0.57	1.32	7.87	0.23	0.44
	CHOS	785	352.12	0.60	1.53	4.30	0.08	0.31
	CHONS	650	362.31	0.88	1.60	3.96	0.34	0.35
	Total	3210	360.04	0.74	1.42	5.56	0.25	0.40
S5 (2017/8/24)	CHO	682	387.23	0.54	1.22	7.79	0.24	0.45
	CHON	1176	396.78	0.65	1.27	7.64	0.26	0.48
	CHOS	677	323.09	0.75	1.50	3.99	0.10	0.35
	CHONS	675	350.81	0.94	1.57	3.98	0.41	0.37
	Total	1987	337.61	0.74	1.38	5.69	0.31	0.43
S6 (2017/8/25)	CHO	528	368.39	0.54	1.17	8.07	0.28	0.48
	CHON	662	352.95	0.66	1.20	7.67	0.36	0.53
	CHOS	447	306.02	0.79	1.53	3.63	0.21	0.34
	CHONS	350	325.54	1.01	1.62	3.47	0.44	0.37

63 Table S2. Relative intensity weighted average values of number, molecular weight ( $MW_w$ ),  
 64 elemental ratios ( $O/C_w$ ,  $H/C_w$ ), double-bond equivalent ( $DBE_w$ ), aromaticity index ( $AI_w$ ), and  
 65  $DBE/C_w$  of different elemental category of assigned formulas in winter.

Samples (Sampling time)	Elemental compositions	Number of Formulars	$MW_w$	$O/C_w$	$H/C_w$	$DBE_w$	$AI_w$	$DBE/C_w$
W1 (2017/12/31 daytime)	Total	1890	293.77	0.61	1.35	5.49	0.30	0.45
	CHO	299	291.00	0.43	0.91	9.01	0.51	0.62
	CHON	587	295.98	0.54	1.09	7.57	0.47	0.60
	CHOS	547	282.56	0.65	1.69	2.72	0.04	0.26
	CHONS	457	317.88	0.85	1.61	3.60	0.33	0.37
	Total	2366	299.72	0.61	1.33	5.60	0.30	0.46
W2 (2017/12/31 nighttime)	CHO	428	293.97	0.46	0.90	8.92	0.51	0.62
	CHON	725	300.06	0.56	1.01	8.04	0.52	0.63
	CHOS	636	288.71	0.64	1.66	2.92	0.05	0.27
	CHONS	577	327.99	0.81	1.59	3.72	0.25	0.36
	Total	1598	289.67	0.59	1.31	5.82	0.34	0.47
W3 (2018/1/1 daytime)	CHO	256	288.65	0.43	0.98	8.41	0.47	0.58
	CHON	477	291.02	0.54	1.11	7.36	0.47	0.59
	CHOS	520	276.16	0.64	1.72	2.52	0.03	0.25
	CHONS	345	314.40	0.89	1.66	3.30	0.36	0.35
	Total	1949	310.34	0.66	1.41	5.24	0.29	0.42
W4 (2018/1/1 nighttime)	CHO	286	310.40	0.42	0.94	9.39	0.50	0.60
	CHON	630	310.82	0.56	1.09	8.10	0.52	0.60
	CHOS	512	292.69	0.56	1.53	3.88	0.11	0.33
	CHONS	521	324.66	0.86	1.64	3.51	0.25	0.35
	Total	2989	294.64	0.67	1.40	5.14	0.31	0.43
W5 (2018/1/8- 2018/1/9)	CHO	564	298.06	0.46	0.92	8.86	0.49	0.61
	CHON	1202	313.36	0.55	1.05	8.15	0.49	0.61
	CHOS	625	272.65	0.67	1.68	2.71	0.05	0.27
	CHONS	601	308.76	0.94	1.63	3.47	0.43	0.37
	Total	4939	321.59	0.60	1.37	5.62	0.27	0.43
W6 (2018/1/19- 2018/1/20)	CHO	878	313.54	0.48	1.02	8.13	0.42	0.56
	CHON	1497	331.31	0.52	1.00	8.74	0.51	0.62
	CHOS	1135	296.52	0.60	1.71	2.78	0.04	0.24
	CHONS	1429	345.52	0.76	1.58	4.08	0.19	0.36

67 Table S3. Classification basis of Van Krevelen diagram.

Classes	H/C	O/C	AI
Lipids-like	$1.7 < \text{H/C} \leq 2.2$	$0 \leq \text{O/C} \leq 0.2$	-
Protein-like	$1.5 < \text{H/C} \leq 2.2$	$0.2 < \text{O/C} \leq 0.6$	-
Lignins-like	$0.6 < \text{H/C} \leq 1.7$	$0.1 \leq \text{O/C} < 0.6$	$\text{AI} < 0.67$
Carbohydrates-like	$1.5 < \text{H/C} \leq 2.2$	$0.6 < \text{O/C} < 1.2$	-
Tannins-like	$0.5 < \text{H/C} \leq 1.5$	$0.6 < \text{O/C} \leq 1.2$	$\text{AI} < 0.67$
Unsaturated Hydrocarbons	$0.7 < \text{H/C} \leq 1.5$	$0 < \text{O/C} < 0.1$	-
Condensed aromatic structure	$0.2 \leq \text{H/C} \leq 0.6$	$0 < \text{O/C} < 0.6$	$\text{AI} \geq 0.67$

68

69 Table S4. Statistics on S-containing compounds based on O/S in summer.

Samples	Number	O/Cw	H/Cw	DBEw	Number	O/Cw	H/Cw	DBEw
CHOS with O/S<4					CHOS with O/S $\geq$ 4			
S1	13	0.61	1.15	9.74	441	0.78	1.53	3.68
S2	11	0.66	1.58	4.37	555	0.76	1.53	3.72
S3	34	0.34	1.61	5.54	885	0.60	1.53	4.11
S4	73	0.24	1.58	7.24	712	0.61	1.53	4.19
S5	28	0.45	1.30	7.63	649	0.75	1.51	3.94
S6	13	0.36	1.56	6.26	434	0.65	1.69	2.69
CHON <sub>1</sub> S with O/S<7 and CHON <sub>2</sub> S with O/S<10					CHON <sub>1</sub> S with O/S $\geq$ 7 and CHON <sub>2</sub> S with O/S $\geq$ 10			
S1	47	0.70	1.25	4.74	373	1.00	1.60	3.77
S2	56	0.72	1.39	3.76	504	0.99	1.66	3.48
S3	138	0.63	1.34	4.42	666	0.84	1.63	3.98
S4	83	0.71	1.28	4.35	567	0.89	1.61	3.94
S5	99	0.71	1.35	4.28	576	0.96	1.59	3.96
S6	41	0.77	1.28	4.11	309	1.03	1.64	3.43

70

71 Table S5. Statistics on S-containing compounds based on O/S in winter.

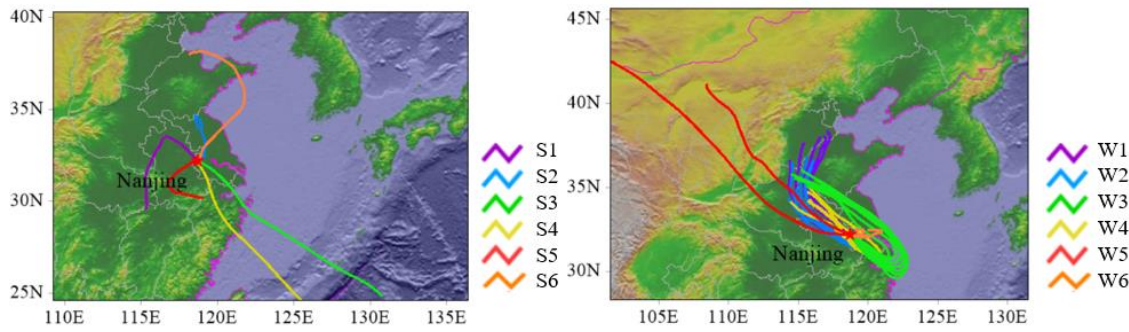
Samples	Number	O/C <sub>w</sub>	H/C <sub>w</sub>	DBE <sub>w</sub>	Number	O/C <sub>w</sub>	H/C <sub>w</sub>	DBE <sub>w</sub>
CHOS with O/S<4					CHOS with O/S≥4			
W1	12	0.40	1.65	2.49	535	0.64	1.66	2.93
W2	8	0.40	1.81	1.82	628	0.64	1.72	2.53
W3	13	0.40	1.65	2.49	507	0.64	1.66	2.93
W4	26	0.36	1.56	6.26	486	0.65	1.69	2.69
W5	12	0.54	1.32	7.75	612	0.80	1.54	3.57
W6	21	0.61	1.71	2.80	1114	0.40	1.91	1.49
CHON <sub>1</sub> S with O/S<7 and CHON <sub>2</sub> S with O/S<10					CHON <sub>1</sub> S with O/S≥7 and CHON <sub>2</sub> S with O/S≥10			
W1	121	0.64	1.32	4.54	336	0.90	1.68	3.37
W2	134	0.65	1.26	4.80	443	0.83	1.65	3.53
W3	79	0.64	1.31	4.56	266	0.93	1.72	3.08
W4	110	0.61	1.30	4.71	411	0.89	1.68	3.36
W5	131	0.65	1.31	4.49	469	0.98	1.68	3.32
W6	386	0.63	1.30	4.95	1043	0.78	1.64	3.91

72

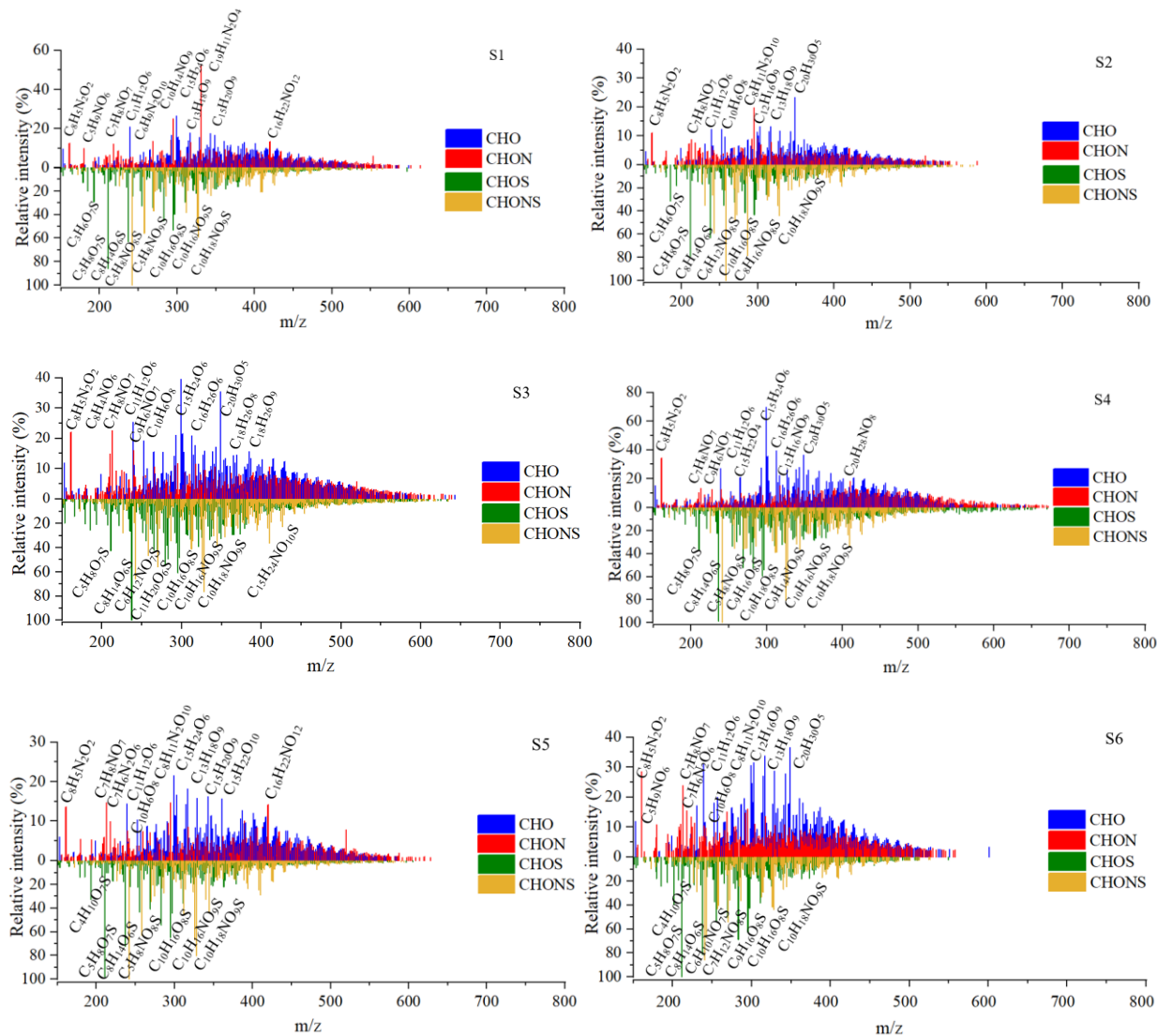
73

74 Figure S1. 48-h backward trajectories in summer (left) and winter (right).

75



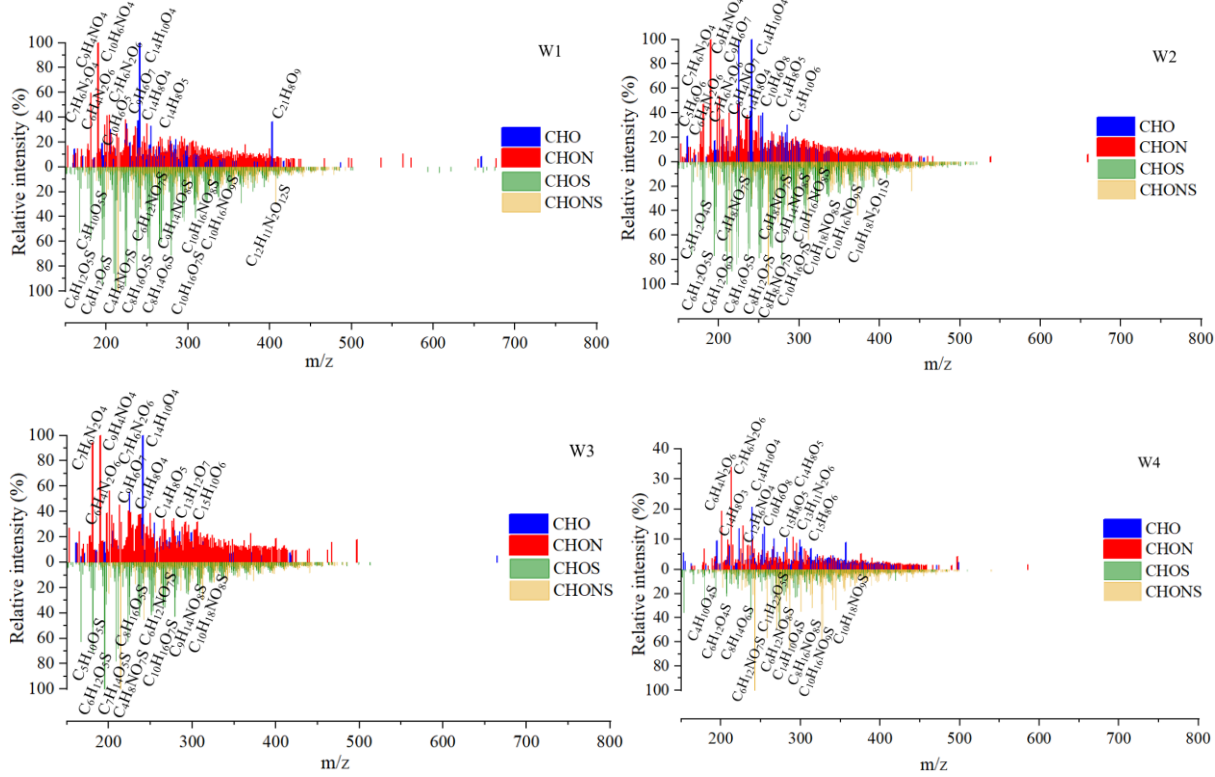
76



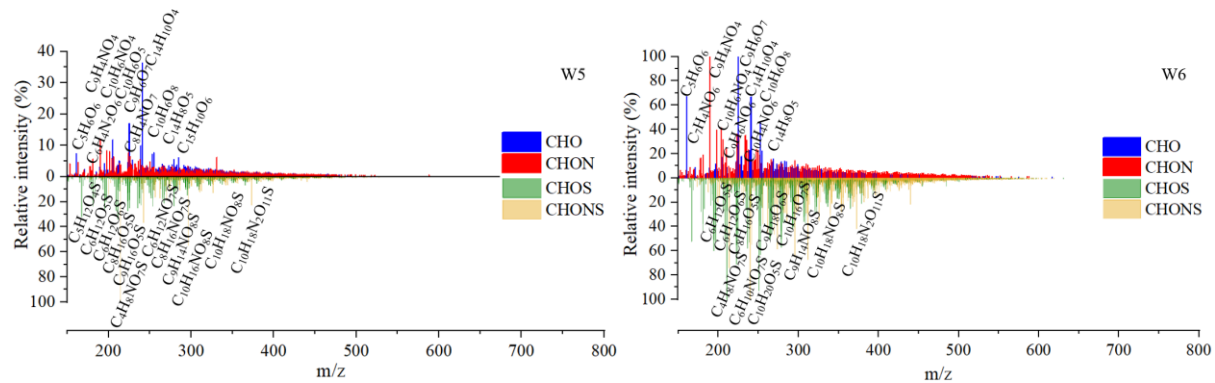
77

78 Figure S2. FT-ICR mass spectra of 6 samples in summer.

80



81

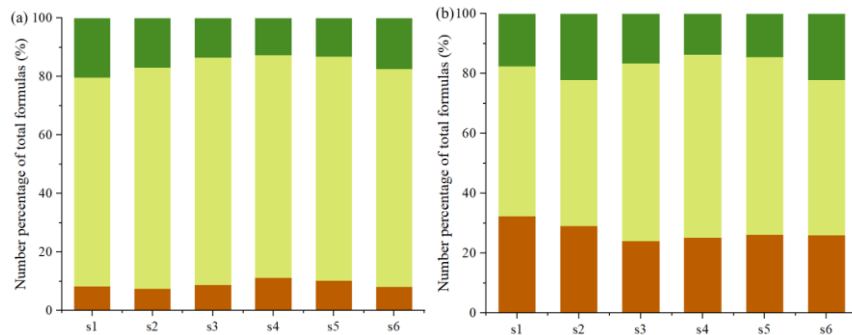


82

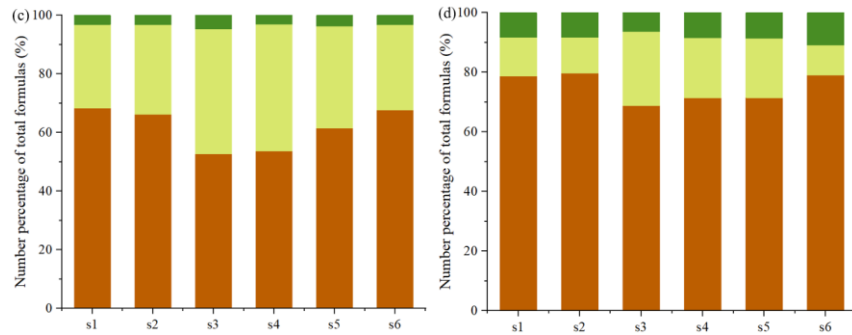
83 Figure S3. FT-ICR mass spectra of 6 samples in winter.

84

Aromatic      Olefinic      Aliphatic



85



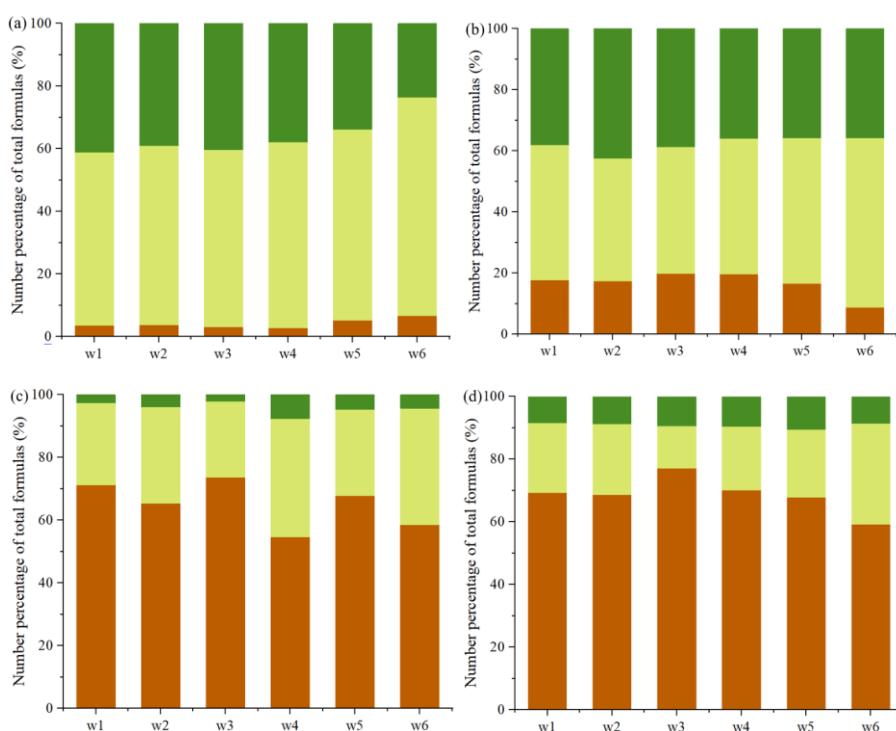
86

87      Figure S4. Number percentage of aliphatic ( $AI=0$ ), olefinic ( $0 < AI \leq 0.5$ ) and aromatic ( $AI > 0.5$ )  
88      formulas in CHO, CHON, CHOS and CHONS compounds in summer.

89

■ Aromatic ■ Olefinic ■ Aliphatic

90

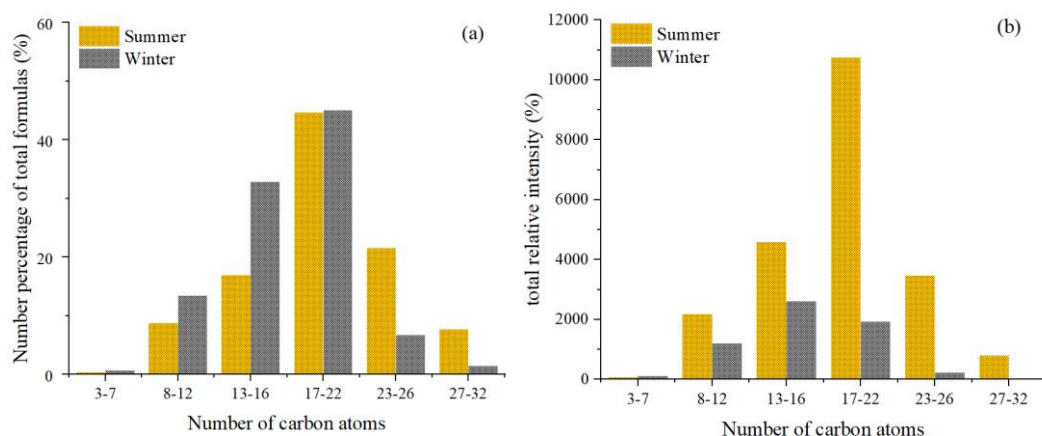


91

92 Figure S5. Number percentage of aliphatic ( $AI = 0$ ), olefinic ( $0 < AI \leq 0.5$ ) and aromatic ( $AI > 0.5$ )  
93 formulas in CHO, CHON, CHOS and CHONS compounds in winter.

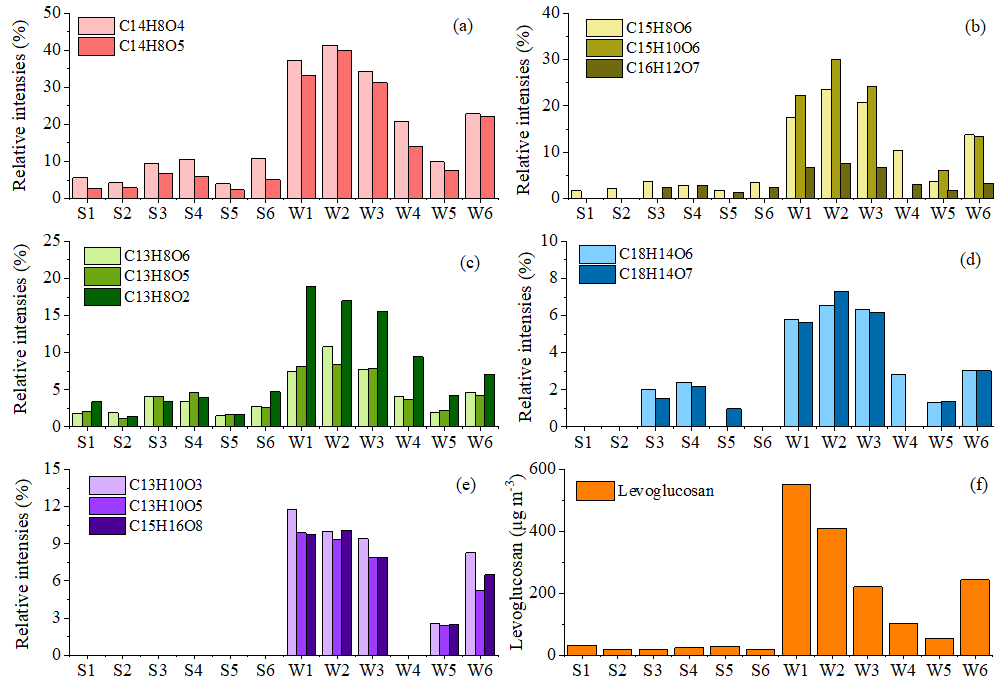
94

95



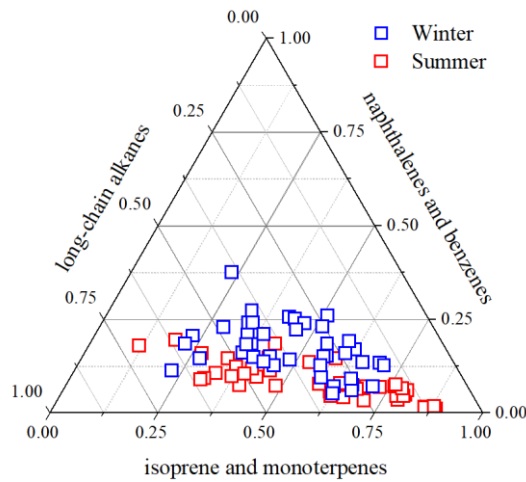
96

97 Figure S6. Number percentage of formulas for different carbon atom numbers (a) and total relative  
98 intensity of formulas for different carbon atom numbers (b) in CHO compounds in summer and  
99 winter.



100  
101  
102  
103  
104  
105

Figure S7. Time series of the relative intensities of typical CHO compounds in biomass burning organic aerosols (BBOA) ((a), (b), (c), (d) and (e)) and the mass concentrations of levoglucosan (f).



106  
107

Figure S8. Distribution of the relative intensities of OSs from different precursors.

- 108 **References**
- 109
- 110 Jiang, H., Li, J., Chen, D., Tang, J., Cheng, Z., Mo, Y., Su, T., Tian, C., Jiang, B., Liao, Y., and  
111 Zhang, G.: Biomass burning organic aerosols significantly influence the light absorption properties  
112 of polarity-dependent organic compounds in the Pearl River Delta Region, China, Environ. Int.,  
113 144, 106079, 10.1016/j.envint.2020.106079, 2020.
- 114 Koch, B. P., and Dittmar, T.: From mass to structure: an aromaticity index for high-resolution  
115 mass data of natural organic matter, Rapid. Commun. Mass. Sp., 20, 926-932, 10.1002/rcm.2386,  
116 2006.
- 117 Kroll, J. H., Donahue, N. M., Jimenez, J. L., Kessler, S. H., Canagaratna, M. R., Wilson, K. R.,  
118 Altieri, K. E., Mazzoleni, L. R., Wozniak, A. S., Bluhm, H., Mysak, E. R., Smith, J. D., Kolb, C.  
119 E., and Worsnop, D. R.: Carbon oxidation state as a metric for describing the chemistry of  
120 atmospheric organic aerosol, Nat. Chem., 3, 133-139, 10.1038/nchem.948, 2011.
- 121 Song, J., Li, M., Jiang, B., Wei, S., Fan, X., and Peng, P.: Molecular characterization of water-  
122 soluble humic like substances in smoke particles emitted from combustion of biomass materials  
123 and coal using ultrahigh-resolution electrospray ionization Fourier transform ion cyclotron  
124 resonance mass spectrometry, Environ. Sci. Technol., 52, 2575-2585, 10.1021/acs.est.7b06126,  
125 2018.